



Generation of color centers by femtosecond laser pulses in wide band gap materials

S. M. Avanesyan,¹ S. Orlando,² S. C. Langford¹, and J. T. Dickinson¹

¹Physics Department, Washington State University, Pullman, WA 99164-2814 USA

²CNR-IMIP/PZ, I - 85050 Tito Scalo (PZ), Italy

ABSTRACT

The high instantaneous powers associated with femtosecond lasers can color many nominally transparent materials. Although the excitations responsible for this defect formation occur on subpicosecond time scales, subsequent interactions between the resulting electronic and lattice defects complicate the evolution of color center formation and decay. These interactions must be understood in order to account for the long term behavior of coloration. In this work, we probe the evolution of color centers produced by femtosecond laser radiation in soda lime glass and single crystal sodium chloride on time scales from microseconds to hundreds of seconds. By using an appropriately chosen probe laser focused through the femtosecond laser spot, we can follow the changes in coloration due to individual or multiple femtosecond pulses, and follow the evolution of that coloration for long times after femtosecond laser radiation is terminated. For the soda lime glass, the decay of color centers is well described in terms of bimolecular annihilation reactions between electron and hole centers. Similar processes appear to operate in single crystal sodium chloride. We report also fabrication of permanent periodic patterns in soda lime glass by two time coincident femtosecond laser pulses.

1. INTRODUCTION

The extremely high power densities associated with femtosecond laser pulses allows for strong nonlinear interactions in nominally transparent materials. Defect production can be exploited to pattern these materials, often with feature sizes smaller than the nominal diffraction limit. Femtosecond lasers have long been exploited to study the kinetics of defect formation on subpicosecond time regimes.¹ If these lasers are to be exploited to modify and pattern transparent materials, the fate of these defects on time scales of nanoseconds to years soon becomes an important issue.

In this work, we examine the fate of defects produced by femtosecond laser radiation on time scales ranging from nanoseconds to hundreds of seconds. For each of two materials, soda lime glass and single crystal sodium chloride, absorption spectroscopy was employed to identify appropriate optically absorbing defects for study. The visible absorption due to these defects was then monitored by measuring the intensity of a CW probe laser of the appropriate wavelength, focused through the center of a spot of material modified by a femtosecond laser.

The rate of darkening during femtosecond irradiation shows complex kinetics that can be modeled in terms of completing defect creation and annihilation. When femtosecond irradiation is stopped, defect annihilation reactions restore a rather large fraction of the transparency lost during irradiation. In the case of soda lime glass, the annihilation reactions can be modeled in terms of bimolecular annihilation of defect centers, probably involving mobile trapped electron centers and stationary trapped hole centers.

In this paper we show that rapid production of diffraction gratings by holographic methods in soda lime glass is easily accomplished.

2. EXPERIMENT

Femtosecond laser pulses were produced by a Spectra Physics Hurricane laser system. The laser source was seeded with a Spectra Physics Mai Tai diode-pumped, mode-locked, Ti:Sapphire laser. After stretching, the pulse was amplified with a Ti:Sapphire regenerative amplifier, pumped with a Spectra-Physics Evolution diode-pumped, Q-switched, Nd:LiYF₄ laser. Subsequent recompression yielded ~1 mJ pulses at 800 nm with a pulse width of 120 fs and a repetition rate of 1 kHz. Frequency doubled and tripled radiation was obtained by directing the 800-nm pulses through appropriately phase matched KDP crystals.

Apparatus for Transmission Measurements

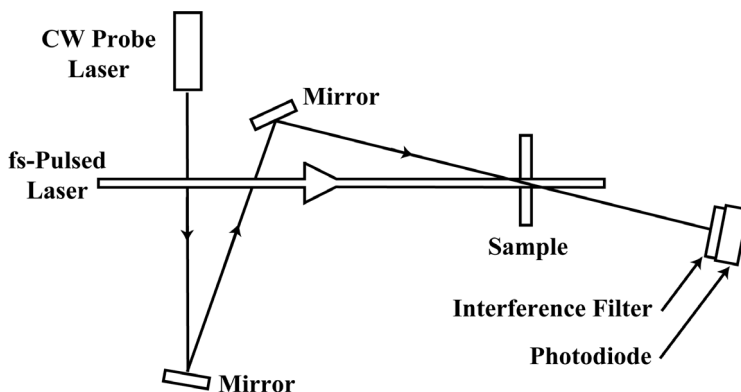


FIG. 1. Experiment to measure transmission of 473-nm light through a soda lime glass sample during exposure to femtosecond laser pulses. The beam of a continuous-wave diode laser is focused through the femtosecond laser spot.

The geometry of the transient absorption measurements is indicated schematically in Fig. 1. The output of the femtosecond laser source was focused with a 1-m focal length lens to form a 0.5 mm diameter spot on the sample. The output of the CW laser was directed obliquely to the femtosecond laser and focused to a 0.1 mm diameter spot at the center of the femtosecond laser spot. CW radiation at 633 nm was provided by a Metrologic Model ML-840 7 mW He:Ne laser. CW radiation at 473 nm was provided by a 10 mW, diode pumped, solid state laser; the intensity of the 473 nm beam was reduced with neutral density filters to avoid transmission changes due to the probe beam. The intensity of the transmitted beam was monitored with a ThorLabs Det 210 high speed photodiode, with a rise time of 1 ns. Interference filters matched to the appropriate CW wavelength minimized signals due to scattered femtosecond radiation. The diode output was digitized and recorded with a LeCroy LC584AXL 1 GHz digital oscilloscope. For maximum sensitivity, an input impedance of 1 M Ω was used in most experiments. Under these conditions, the RC time constant of the detection electronics was about 130 μ s. For fast time scale measurements at reduced sensitivity, RC time constants of about 10 ns could be obtained with an input impedance of 50 Ω .

Absorption spectra in the visible and ultraviolet regions were acquired with a Perkin Elmer Lambda 9000 spectrophotometer. Light transmitted through the sample was collected in a Spectralon integrating sphere equipped with an extended range photomultiplier tube and a thermostated PbS detector. The use of an integrating sphere insures that forward-scattered light transmitted through the sample was properly detected and included in the measured transmission.

The samples employed in this work include soda lime glass slides (Gold Seal[®] microscope slides, Portsmouth, New Hampshire, USA) and infrared-grade single-crystal sodium chloride (International Crystal Labs, Garfield, New Hampshire, USA).

3. RESULTS

3.1. Soda lime glass

Absorption spectrum. The absorption spectrum of soda lime glass darkened with femtosecond laser radiation is similar to the absorption spectra of glass darkened with x- and γ -rays. Figure 2 displays the absorbance [$\log_{10}(I/I_0)$] of an as-received, 1-mm thick soda lime glass slide prior to irradiation, along with glass slides darkened with 800-nm femtosecond laser pulses and Cu K α x-ray radiation from an x-ray diffraction unit. The spectral features in both darkened materials are stable on time scales of months. The broad absorption peaks centered at 460 and 620 nm are quite similar to absorption peaks observed in pure, x-irradiated soda silicate glasses^{2,3} and soda aluminosilicate glasses.⁴ Both femtosecond- and x-irradiated glasses also show enhanced absorption in the near UV due to trapped electron centers.^{2,3} Color center formation in alkali silicates by exposure to ultrafast laser pulses at 850 nm has been previously reported and attributed to the response of the glass to the short wavelength component of supercontinuum light.⁵ We find coloration occurring at laser intensities well below any white light formation and are able to explain defect formation as being initiated by multiphoton excitation.

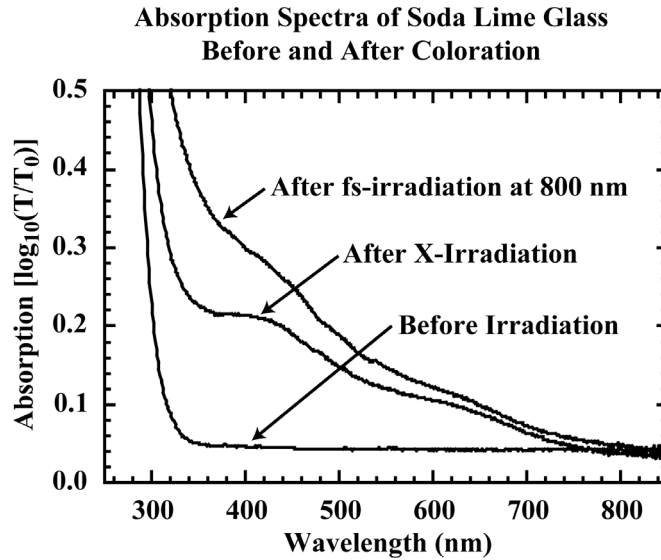


FIG. 2. UV-VIS absorption spectra of untreated soda lime glass, of glass exposed to femtosecond 800-nm radiation, and glass exposed to Cu K α x-rays. The broad peaks at 420 nm and 620 nm are attributed to H $_2^+$ and H $_3^+$ trapped-hole centers, respectively.

The broad absorption at 460 nm is conveniently probed with commercial CW diode lasers. In this work, the beam from a 473 nm diode laser was focusing through the center of the femtosecond laser spot. The transmitted intensity was measured with a fast photodiode.

Evolution of color center formation during fs irradiation. The coloration produced by femtosecond laser radiation is a strong function of pulse energy.⁶ The transmission of 473-nm probe signal through an initially clear soda lime glass slide during exposure to 400-nm pulses (1 kHz repetition rate) appears in Fig. 3 for five pulse energies. Irradiation started at time $t = 0$ and continued for the duration of data collection. As one might expect, the transmission drops rapidly at high pulse energies and slowly at low pulse energies.

Transmission of 473 nm Probe Beam through Soda Lime Glass during Irradiation with fs Pulses at 400 nm

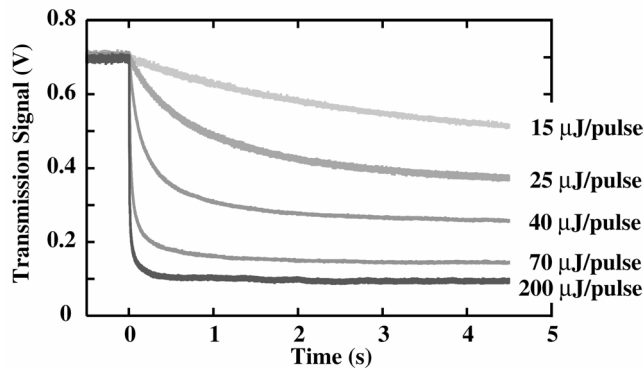


FIG. 3. Transmission at 473 nm through soda lime glass during exposure to 400-nm femtosecond laser pulses at five selected pulse energies. One thousand femtosecond pulses per second were directed at the sample starting at time $t = 0$.

On the time scale of seconds, the transmission changes smoothly with time. High time-resolution measurements show clear, step-like drops with each laser pulse, especially at high pulse energies. Transmission measurements during the first five high-intensity femtosecond pulses incident on a soda lime glass slide on millisecond time scales (1 M Ω input resistance) are reported in Fig. 4(a). A nanosecond time scale measurement of the transmission signal during the first femtosecond pulse is shown in Fig. 4(b) (50 Ω input resistance). On both time scales, the initial drop in the transmission signal is rate limited by the time constant of the detection electronics. The nanosecond-scale transmission measurements show that the initial transmission drop is faster than about 10 ns. This is comparable to the 10 ns response of the electronics to a femtosecond pulse, shown in the inset of Fig. 4(b).

Transmission of 473 nm Probe through Soda Lime Glass at Onset of 400 nm fs Laser Irradiation at 200 μ J/pulse

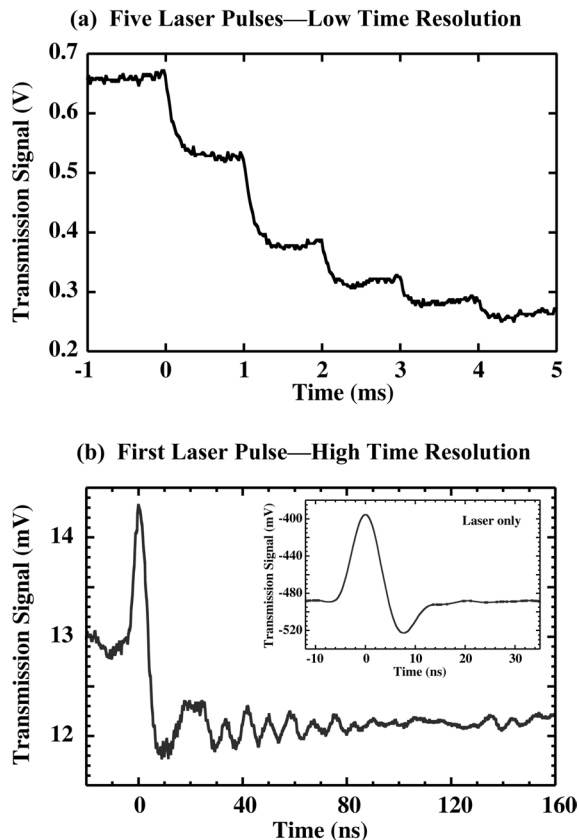


FIG. 4. Transmission at 473 nm during exposure to 400-nm femtosecond pulses at 200 μ J/pulse. (a) Transmission during the first five laser pulses acquired with 1 M Ω input impedance (time resolution about 130 μ s). (b) Average transmission signal acquired with an input impedance of 50 Ω (time resolution about 10 ns). The inset in (b) shows the signal due to scattered laser femtosecond laser light (no probe); scattered light is responsible for the peak in the transmission signal coincident with the laser pulse in (b).

Although defect creation is instantaneous on the time scale of these measurements, the transmission signal shows interesting kinetics between femtosecond pulses—provided that the total defect density is sufficiently high. The transmission drop following the first laser pulse in Fig. 4(a) is essentially permanent on the millisecond time scale. However, the transmission accompanying subsequent pulses drops immediately after the femtosecond pulse, then gradually rises until the next femtosecond pulse. Eventually an equilibrium is reached where the transmission drop produced by a femtosecond pulse has entirely recovered just prior to the next femtosecond pulse.

The transmission rise between femtosecond pulses is especially evident in the microsecond time scale measurements of Fig. 5. After a few microseconds, transmission increases almost half-way back to its value before the

femtosecond pulse. Significantly, the transmission rise or recovery is subsequently proportional to $t^{1/2}$, where t is the time since the most recent femtosecond pulse. This functional behavior is characteristic of bimolecular annihilation, where two defects (one mobile) annihilate when the mobile defect encounters its immobile partner. The $t^{1/2}$ time behavior in particular suggests that the mobile defect executes a random walk along a line or linear structure. As discussed below, this behavior is reasonable in light of the structure of alkali silicate glasses.

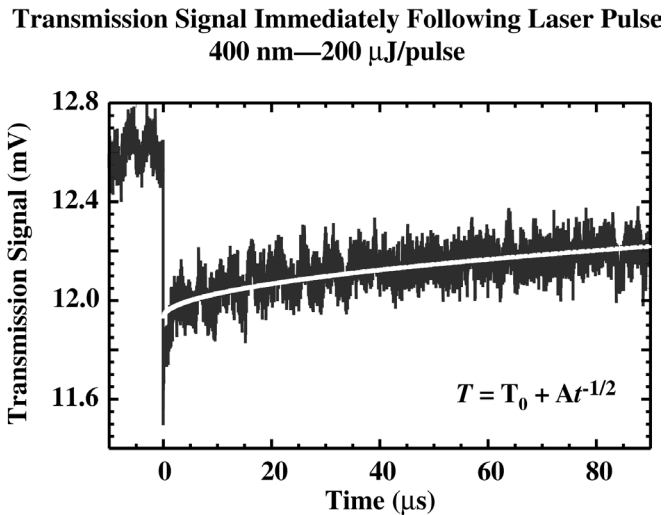


FIG. 5. Average transmission signal acquired with an input impedance of 50Ω (time resolution about 10 ns), showing the initial stages of transmission recovery following each pulse. The light line through the data shows a least squares fit of the data to a square-root decay.

Recovery of Transmission thru Soda Lime Glass
at 633 nm after Exposure to 80,000 Femtosecond Pulses
at 930 $\mu\text{J}/\text{pulse}$

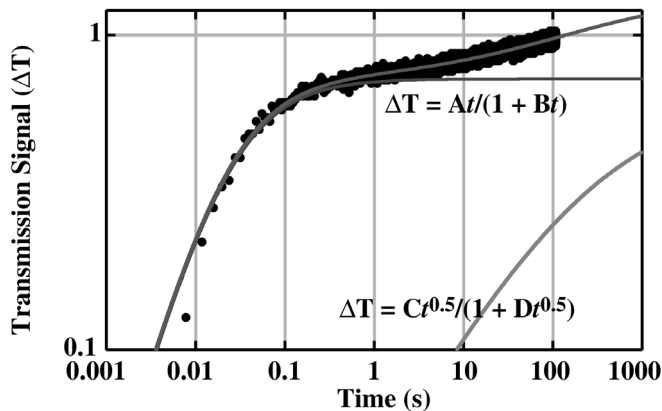


FIG. 6. Recovery of the transmission signal after a darkening experiment plotted on a log-log scale. Darkening was achieved by exposure to 800-nm femtosecond laser radiation for 80 s with 1000 pulses per second at 930 μJ per pulse. The femtosecond laser beam was blocked at time $t = 0$ and remained blocked for the remainder of data collection. The signal at time $t = 0$ has been subtracted from each data point to emphasize the initially rapid recovery of the signal. The broad gray line shows the best fit of the data to a model incorporating Eqs. (2) and (5). This model represent the sum of two bimolecular annihilation processes, one where the mobile species is free to move in three dimensions and the other where the mobile species is confined to one dimensional structures.

Modeling transmission recovery. Transmission recovery continues for hundreds of seconds, as shown in Fig. 6. This particular sample was colored with 80,000 pulses of 800-nm femtosecond light, and was probed in the 620 nm absorption band with a 633-nm He:Ne laser. Here, time $t = 0$ corresponds to the onset of recovery, when the femtosecond laser beam was blocked. In contrast with the transmission recovery on microsecond time scales, the recovery between 10 ms and 1 s is well described by bimolecular annihilation on a three dimensional lattice: the mobile defect is free to move in all three dimensions. We assume reactions of the form $A + B \rightarrow 0$, where the concentration of species A equals the concentration of species B. Typically, one assumes that one defect is mobile and performs a random walk on a lattice of L distinct sites, where some of the sites are occupied stationary recombination centers B. The probability (per unit time) of a walker encountering a recombination center is the product of the fraction of sites occupied by recombination centers (N/L), the average number of distinct sites visited by the walker per unit time S , and the total number of walkers (N). For uniform lattices (for example, cubic lattices where the jumping probability is identical for all pairs of adjacent sites) the average number of distinct sites visited by a walker per unit time is constant for all lattice dimensions $D > 2$. Then

$$\frac{dN}{dt} = -\left(\frac{N}{L}\right)SN = -\frac{S}{L}N^2 \quad (1)$$

The solution of this equation takes the form:

$$N(t) = \frac{N_0}{1 + CN_0 t} \quad (2)$$

If the mobile species is confined to structures of dimension *less* than two, the average number of sites per unit time visited by a walker is not constant. For instance, the average number of sites visited in a random walk along a 1-D line is proportional to $t^{1/2}$, because the walker spends much of its time visiting previously visited sites. Since the walker must have survived its passage through these previously visited sites, it is safe during subsequent visits to the same sites. In soda lime glass, some mobile defects may be confined to linear channels of sodium ions and their associated nonbonding oxygen centers. The existence of such channels is predicted by molecular dynamics simulations⁷⁻¹¹ and has been verified by x-ray diffraction¹² and magnetic resonance studies.¹³

Under these conditions, the probability of encountering new sites is proportional to the derivative of the total number of distinct sites visited, so $S = (S'/2) t^{1/2}$, with S' a constant. The probability S can vary in similar ways if the mobile species encounters electron traps with a distribution of trap depths, where the mobile species spends a disproportionate time at sites with deep traps. If $S(t)$ scales with the inverse square root of time, Eq. (1) becomes

$$\frac{dN}{dt} = \frac{-S't^{-1/2}}{2L}N^2 \quad (3)$$

Equation (3) is readily solved by changing the variable of integration to $f = t^{1/2}$. Expressing N in terms of f yields:

$$\frac{dN}{df} = -\frac{S'}{L}N^2 \quad (4)$$

The solution of Eq. (4) is formally the same as the solution of Eq. (1), with $t^{1/2}$ replacing t . More generally, for dimensions less than two, the average total number of sites visited by a walker is proportional to $t^{D/2}$,¹⁴ and

$$N(t) = \frac{N_0}{1 + CN_0 t^{D/2}} \quad (5)$$

where $C = S'/L$. This non-integral time behavior is often described as “fractal time.”

The kinetics of transmission recovery in soda lime glass are well described in terms of recombination on 1-D and 3-D lattices, corresponding to terms with t^1 from Eq. (2) and $t^{1/2}$ in Eq. (5) (with $D = 1$). Extrapolating these equations to long times, using best fit parameters, suggests that approximately 30% of the defects present at the end of femtosecond irradiation are permanently stable. Physically, these defects constitute a separate population of defects that do not participate in the annihilation reactions described above. For instance, these defects may be physically isolated from mobile species.

In the short time limit, the $t^{1/2}$ term in Eq. (5) (for $D = 1$) dominates the t^1 term in Eq. (2). The curve fit parameters obtained from the data of Fig. 6 indicate that the $t^{1/2}$ term dominates at times less than a few microseconds. This is consistent with the early time behavior of the transmission recovery in Fig. 5, especially considering the vastly different experimental conditions employed in the two experiments.

3.2. Sodium chloride

Darkening kinetics. Femtosecond pulses also color the alkali halides at modest pulse energies. The absorbance of a typical sodium chloride crystal before and after darkening by 400 nm femtosecond radiation is shown in Fig. 7. The broad F-center peak at 460 nm is well situated for probing at the 473 nm wavelength of the blue diode laser. The F-center consists of an alkali vacancy associated with a trapped electron. Thus the F-center site has the same nominal charge as the same site without the defect. F-center formation in the alkali halides has been extensively studied,¹⁵⁻¹⁹ providing a wealth of information to use in the interpretation of new results. The other peaks in the absorption spectrum of Fig. 7 are attributed to M-centers (formed by two F-centers on adjacent sites) and V-centers (miscellaneous hole traps, often associated with impurities).

Absorption Spectra of NaCl Before and After Darkening by 400 nm Femtosecond Laser Pulses

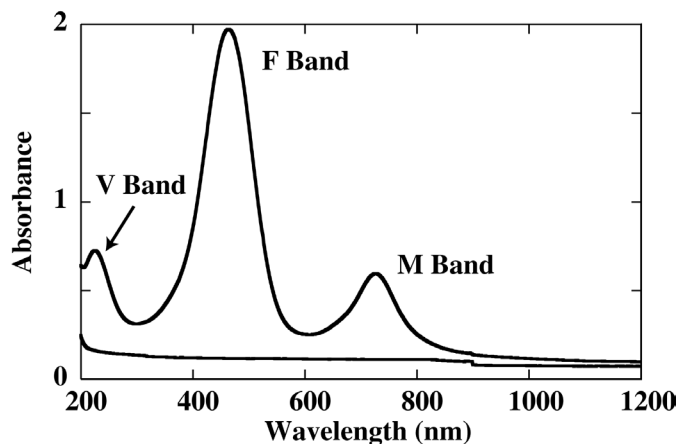


FIG. 7. Absorption spectra of a sodium chloride sample before and after darkening by 400-nm, femtosecond laser irradiation.

Transmission of 473 nm Probe through Single Crystal NaCl during fs-Laser Irradiation at 400 nm

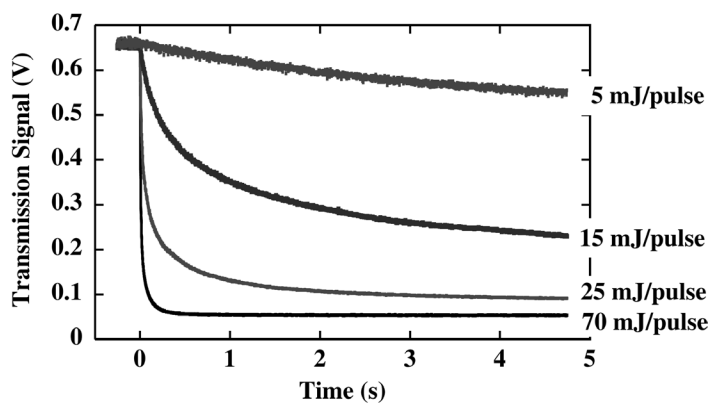


FIG. 8. Transmission at 473-nm through single crystal sodium chloride during femtosecond laser irradiation at 400-nm at four different pulse energies.

The progress of darkening during irradiation with 400-nm femtosecond pulses at four distinct pulse energies is illustrated in Fig. 8. As with soda lime glass, the rate of darkening is a strong function of pulse energy. At high pulse energies, the transmission at 473 nm quickly reaches an apparent minimum.

Model of transmission change during darkening. A model of the darkening process can be constructed by incorporating a defect source term into the equations for bimolecular annihilation. If the number of defects produced per laser pulse is the same for each laser pulse ($= A$), then $N = N + A$ immediately after each pulse. The bimolecular annihilation reaction of Eq. (1) operates between femtosecond pulses. In practice, it is convenient to work with more continuous functions, for example:

$$\frac{dN}{dt} = A - CN^2 \quad (6)$$

The interpretation of the constants A and C in Eq. (8) is not straightforward due to the nature of the averaging process. Incorporating initial conditions [$N(t=0) = 0$], the solution can be expressed as:

$$N(t) = \sqrt{\frac{A}{C}} \tanh(\sqrt{AC} t) \quad (7)$$

Although this solution displays the correct behavior in the long time limit, the predicted initial rate of darkening is much faster than that the observed rate. A good fit to the experimental data is obtained by raising the time to a fractional power:

$$N(t) = \sqrt{\frac{A}{C}} \tanh(\sqrt{AC} t^M) \quad (8)$$

where $M \neq 1$, i.e., fractal time. The need for fractal time in this continuum model may result treating discrete defect creation events (with each femtosecond pulse) as a continuous process. Models that incorporate defect creation and annihilation with each laser pulse are under construction and we hope to resolve this point soon.

Signal due to 473 nm Probe Transmitted through Single Crystal NaCl as a Function of Time after the Onset of 400 nm fs Laser Irradiation

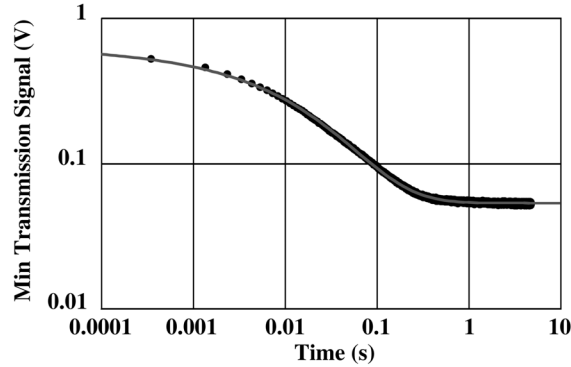


FIG. 9. Log-log plot of the 473-nm transmission signal through single crystal sodium chloride during exposure to 400-nm, 70 μ J femtosecond pulses. The curve represents a least squares fit of Eq. (8) to the data, representing bimolecular annihilation where the mobile species is free to move in all three dimensions.

A log-log plot of a least squares fit of Eq. (8) to 473-nm transmission data acquired at a femtosecond pulse energy of 70 μ J is shown in Fig. 9. Equation 10 provides a good fit to the data over five orders of magnitude in time. Similar fits were obtained for pulse energies from 10 to 200 μ J. Although the data are limited, the parameters corresponding to $(A/C)^{1/2}$ and $(AC)^{1/2}$ are consistent with defect production by a multiphoton process, where the defect production parameter A scales as a power of the pulse energy of at least two and C remains approximately constant. The power M in Eq. (8) is approximately 0.3 over this range of pulse energies. If this interpretation of A and C is correct, we should be able to fit data acquired at other pulse energies with the same C parameter; A should scale with the pulse energy to the third power (the expected pulse energy dependence).

Signal due to 473-nm Probe Beam through Soda Lime Glass during fs-Irradiation at 400 nm, 70 μ J/pulse

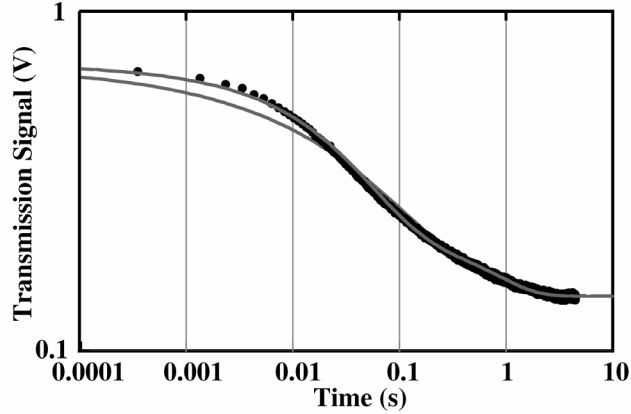


FIG. 10. Log-log plot of the transmission at 473-nm through soda lime glass during exposure to 400-nm, 70- μ J, femtosecond pulses. The lower light line shows a least squares fit of Eq. (8) to the data. The upper light line shows a least squares fit of two terms corresponding to Eqs. (8) and (9), for the case $M = 1$.

Equation (8) is less successful at describing the darkening process in soda lime glass. A log-log plot of a least squares fit of Eq. (8) to typical transmission data during darkening is shown by the lower gray line in Fig. 10. The fits falls well below the data at times below 100 ms. If defect recombination evolves independently on 1-D and 3-D lattices, as suggested by the recovery of transmission after femtosecond irradiation, one might expect the darkening process to involve two independent processes as well. This would involve two defect densities, each with its own absorption and time evolution described by Eq. (8). Dimensionally, one expects the time exponent for a 3-D lattice to be twice the exponent for a 1-D lattice; that is, the time evolution of the defect density on the 1-D lattice would take the form:

$$N(t) = \sqrt{\frac{A'}{C'}} \tanh(\sqrt{A'C'} t^{M/2}) \quad (9)$$

Curve fits employing independent terms combining Eqs. (8) and (9) suggest that M is very close to one. A combined curve fit with M set to 1 is plotted in Fig. 10 (upper light curve, four free parameters) and provides good fit to the data at short times.

Although full understanding of defect production and annihilation in these materials during femtosecond irradiation is still lacking, a consistent picture is emerging in the case of soda lime glass. Models that treat defect annihilation in terms of bimolecular recombination operating independently on 3-D and 1-D sublattices provide a good description of the data. Physically, the 1-D sublattice would correspond to sodium-rich channels in this material. The situation is less clear in the case of sodium chloride. Preliminary data suggests that we may need to account for charge exchange among defects during femtosecond radiation to fully account for the darkening and recovery processes.

4. GRATING FORMATION

Creation of gratings inside the transparent materials by multiphoton nonlinear effects could have potential applications in integrated optics and photonics²⁰⁻²². Highly nonlinear effects similar to the darkening in soda lime glass are often useful for patterning transparent materials. We can pattern a grating using this darkening mechanism with femtosecond, 800 nm laser pulses by splitting the beam into two equal intensity beams that are allowed to interfere at angle θ . Figure 11 shows the center and higher order spots out to fourth order produced when the 633 nm beam from a He:Ne laser is diffracted by a grating produced by the interference of two femtosecond, 800 nm laser beams converging at an angle $\theta=1.3^\circ$. This geometry is expected to produce dark strips with spacing $\Lambda=\lambda/2\sin(\theta/2)$, where λ is the wavelength used to write the pattern. The predicted grating spacing is therefore $\Lambda=35 \mu\text{m}$. The diffraction pattern displayed in Fig.11 is consistent with $\Lambda=36 \mu\text{m}$, in agreement with the predicted value. The radiant intensity in the diffracted beams makes up 10.5% of the total intensity transmitted.

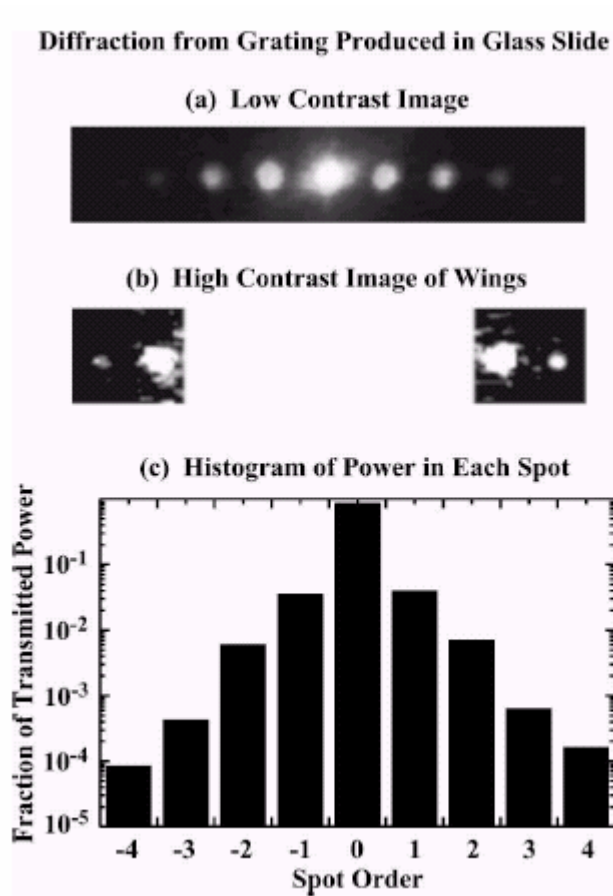


FIG. 11. (a) Low contrast image of a diffraction pattern produced by the diffraction of a cw He:Ne beam from a grating produced in a soda lime glass slide by femtosecond pulses of 800 nm radiation. (b) High contrast image showing higher order spots. (c) Histogram of the fraction of the total transmitted power found in each spot of the diffraction pattern.

5. CONCLUSION

Defects generated by femtosecond laser pulses in soda lime glass and sodium chloride produce a persistent coloration that can be stable for very long times. In each case, the rate of defect formation during exposure depends strongly on the pulse energy. The competition between defect creation and annihilation complicates the kinetics of darkening. When femtosecond laser irradiation ceases, only annihilation operates, resulting in simpler kinetics. The kinetics of defect annihilation in soda lime glass appear to be affected by the unusual molecular structure of this material, which includes linear channels of alkali ions surrounded by nonbonding oxygen centers. Analysis of the recovery kinetics suggests that about 30% of the defects present at the end of femtosecond irradiation in soda lime glass persist in the long time limit. An understanding of defect creation and annihilation is necessary to ensure that pattern formation in transparent material displays the desired degree of persistence.

Finally, we show that pattern formation (gratings) in soda lime glass with a diffraction efficiency $\sim 10\%$ can be readily achieved.

Acknowledgments

This work was supported by the Department of Energy under Contract Number DE-FG03-98ER14864, by a Major Research Instrumentation Grant from the National Science Foundation under Contract Number DMR 00-79774 and by CNR-NATO Senior Fellowships Programme 2001 (Grant no. 217.34)

References

1. N. Bloembergen, *Rev. Mod. Phys.* **71**, S283-S287 (1999).
2. J. H. Mackey, H. L. Smith, and A. Halperin, *J. Phys. Chem. Solids* **27**, 1759-1772 (1966).
3. A. J. Cohen and G. G. Janezic, *Phys. Stat. Solidi (a)* **77**, 619-624 (1983).
4. G. H. Sigel, Jr., *J. Non-Cryst. Solids* **13**, 372-398 (1973/74).
5. O. M. Efimov, L. B. Glebov, S. Grantham, and M. Richardson, *J. Non-Cryst. Solids* **253**, 58-67 (1999).
6. J. B. Lonzaga, S. M. Avanesyan, S. C. Langford, and J. T. Dickinson, *J. Appl. Phys.* **97**, 4332-4340 (2003).
7. T. F. Soules, *J. Chem. Phys.* **71**, 4570-4578 (1979).
8. S. K. Mitra and R. W. Hockney, *Philos. Mag. B* **48**, 151-167 (1983).
9. R. A. Murray and W. Y. Ching, *J. Non-Cryst. Solids* **94**, 144-159 (1987).
10. R. G. Newell, B. P. Feuston, and S. H. Garofalini, *J. Mater. Res.* **4**, 434-439 (1989).
11. C. Huang and A. N. Cormack, *J. Chem. Phys.* **93**, 8180-8186 (1990).
12. G. N. Greaves, A. Fontaine, P. Lagarde, D. Raoux, and S. J. Gurman, *Nature* **293**, 611-616 (1981).
13. R. Dupree, D. Holland, and D. S. Williams, *J. Non-Cryst. Solids* **81**, 185-200 (1986).
14. G. Zumofen, A. Blumen, and J. Klafter, *J. Chem. Phys.* **84**, 6679-6686 (1986).
15. F. Seitz, *Rev. Mod. Phys.* **26**, 7-94 (1954).
16. *Physics of Color Centers; Vol.*, edited by W. B. Fowler (Academic Press, Boston, 1968).
17. E. Sonder and W. A. Sibley, in *Point Defects in Solids*, edited by J. Crawford, James H. and L. M. Slifkin (Plenum, New York, 1972), p. 201-290.
18. N. Itoh, *Adv. Phys.* **31**, 491-551 (1982).
19. N. Itoh and M. Stoneham, *Materials Modification by Electronic Excitation* (Cambridge University, Cambridge, UK, 2000).
20. Ken-ichi Kawamura, Nobuhiko Sarukura, Masahiro Hirano, Naoko Ito, Hideo Hosono, *Appl. Phys. Lett.* **79**, 1228 (2001).
21. Yan Li, Wataru Watanabe, Kazuhiro Yamada, Taishi Shinagawa, Kazuyoshi Itoh, Junji Nishii, Yongyuan Jiang, *Appl. Phys. Lett.* **80**, 1508 (2002).
22. Toshio Kurobori, Tetsu Kitao, Yukio Hirose, Ken-ichi Kawamura, Daijyu Takamizu, Masahiro Hirano, Hideo Hosono, *Radiation Measurements* (2004), available online at www.sciencedirect.com